SINTEF

This is the Accepted version of the article

Metal films for MEMS pressure sensors: comparison of Al, Ti, Al-Ti alloy and Al/Ti film stacks

Elizaveta Vereshchagina, Erik Poppe, Kari Schjølberg-Henriksen, Markus Wöhrmann, Sigurd Moe

Citation:
Elizaveta Vereshchagina, Erik Poppe, Kari Schjølberg-Henriksen, Markus Wöhrmann, Sigurd Moe(2018) PMetal films for MEMS pressure sensors: comparison of Al, Ti, Al-Ti alloy and Al/Ti film stacks. 2018 7th Electronic System-Integration Technology Conference (ESTC), Dresden, Germany, 18-21 Sept. 2018
DOI: 10.1109/ESTC.2018.8546422

This is the Accepted version.
It may contain differences form the journal's pdf version

This file was downloaded from SINTEFs Open Archive, the institutional repository at SINTEF
http://brage.bibsys.no/sintef

Metal films for MEMS pressure sensors: comparison of Al, Ti, Al-Ti alloy and Al/Ti film stacks

Elizaveta Vereshchagina
SINTEF Digital
Department of Microsystems and Nanotechnology
Oslo, Norway
Elizaveta.Vereshchagina@sintef.no

Erik Poppe
SINTEF Digital
Department of Microsystems and Nanotechnology
Oslo, Norway

Kari Schjølberg-Henriksen
SINTEF Digital
Department of Microsystems and Nanotechnology
Oslo, Norway

Markus Wöhrmann
Fraunhofer IZM
Department WLSI
Berlin, Germany

Sigurd Moe
SINTEF Digital
Department of Microsystems and Nanotechnology
Oslo, Norway

***Abstract*—Thermo-mechanical stability of metal structures is one of the key factors affecting accuracy of micro-electromechanical (MEMS) piezoresistive pressure sensors. In this work, we present the measurement results of stress and hysteresis for the following metals deposited in the same sputtering equipment – Al, Ti, Al-Ti alloy and stacks of Al/Ti films – enabling, for the first time, a direct comparison between their thermo-mechanical properties supported with analysis of surface morphology (grain size, hillocks and voids).**

Keywords—Metallization, thermo-mechanical stress, thermal hysteresis, aluminium, aluminium-titanium alloy, pressure sensor

I. Introduction

The introductory section is divided into four parts. First, the effects of thermo-mechanical stress and hysteresis due to the presence of metal structures are explained. This followed by a brief overview of the methods that can be used for both wafer-level and sensor-level stress characterization. Next, surface and structural changes in metal films due to the thermo-mechanical stress are addressed. Finally, a summary of the objectives for this work is provided.

A. Thermal hysteresis and drift

Metal microstructures are required in most of the MEMS sensors and actuators. The difference in thermo-mechanical properties between metal films, silicon substrate and other commonly used thin films (oxides, nitrides, poly-Si, etc.) unavoidably affects the sensor performance and must be accounted for during all stages of the sensor development. Therefore, control and reduction of drift in sensor signal due to the hysteresis of thermo-mechanical stress is among the most challenging and critical issues to address in MEMS-based pressure sensor technology [1-4].

Al is one of the most widely used and studied metallization materials in various stress-sensitive MEMS. The residual stress measured at room temperature in the Al-Si wafer is caused by both mismatch between the Al and the Si substrate during thermal expansion, and an effect of the Al microstructure (intrinsic stress after deposition). Above 100–150 °C, Al typically exhibits a non-linear thermo-mechanical behavior, i.e. thermal hysteresis. This is due to a sufficiently high mobility in the Al thin film at these temperatures leading to relaxation of stress by changes on the microstructural level, e.g. grain growth and hillocks/voids formation [3-7].

Thermal hysteresis is a measurable difference in sensor output under the same operating conditions and external impulse after heating and cooling is applied. High reliability and high accuracy applications of pressure sensors, e.g. avionics, automobile and medical industries, require good control over signal drift due to the thermal hysteresis. The phenomenon of hysteresis, among other device-specific factors, is dependent on the non-linear thermo-mechanical behavior of metal thin films comprising the system, thermal history of a device, metal deposition equipment and process parameters [5-8]. Through quantitative analysis of residual stress and hysteresis it is possible to understand its causes, to identify the temperature range within which its influence is minimal, and, possibly, to determine the most suitable deposition processes and designs, ultimately leading to improved sensor reliability.

Even though properties of Al films are well reviewed in the literature there is still lack of quantitative data about hysteresis of thermo-mechanical stress and alternatives to reduce it within the temperature range relevant for pressure sensing technology, i.e. from room temperature (RT) to 200 ˚C. Several approaches to thermal hysteresis reduction, mainly combining the effect of thermal loading on sensor output with finite element method (FEM), were demonstrated in the literature [1-4]. These approaches, however, require complex sensor processing and packaging, and, thus, excessive costs, if several metal alternatives need to be screened. Moreover, during testing the stress induced by packaging cannot be excluded. The wafer-level stress measurement techniques in combination with thermal cycling, discussed in the following section, can be a useful, complimentary tool to study stress and stress hysteresis and provides data that can be, in contrary to most of the studies on complete sensor elements, directly used by others.

To the best of our knowledge, this work provides for the first time the comparative data on stress and stress hysteresis

This work is funded through the Norwegian Research Council through the project NBRIX (247781).

XXX-X-XXXX-XXXX-X/XX/$XX.00 ©20XX IEEE

for Al, Ti, Al-Ti stack and Al-Ti (1.8% Ti) alloy deposited in the same equipment. In addition, the surface properties and the integration aspects of these metals are discussed. This data can be used in evaluation of alternative metal films for various stress-sensitive MEMS applications.

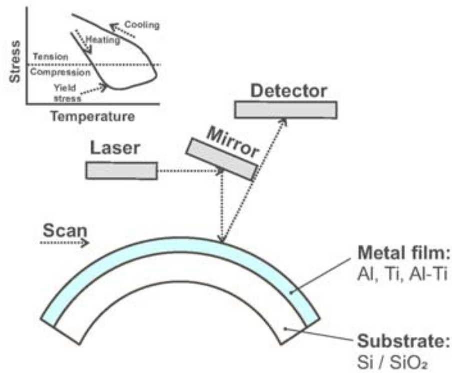

Fig. 1. Schematic of the measurement principle relying on the laser level technique. The laser beam is reflected from the wafer surface and the deviation is used for the calculation of warpage using Stoney's equation (Eq.1)

B. *Characterization of stress-temperature behaviour of thin metal films*

Investigation of temperature-related stress effects on the wafers scale can be carried out by wafer curvature (warpage) analysis, X-ray diffraction (XRD), White Light Interferometry (WLI) and ellipsometry techniques. The stress measurement method selected for this study – warpage analysis – does not require detailed prior knowledge about properties of the deposited metal films, only its thickness. It allows quantification of thermal hysteresis and stress relaxation mechanisms, as well as establishing the relationship between the residual stresses, deposition parameters and thermal history of wafers. The wafer warpage technique is well suited for studying the effect of integration of a thin capping film of Ti (Al-Ti stacks) and use of Al-Ti alloys as alternative metal systems to standard Al metallization, which are among the main goals of this study. A possible drawback of wafer warpage analysis is relatively long times required for completion of thermal cycling experiments. As the measurement method is differential, the influence of substrate must be eliminated by additional cycling experiment prior to metal deposition or after etching the studied metal film. Advances in the XRD characterization technique also allow accurate quantification of strains in situ at elevated temperatures [9-12]. Contrary to the warpage analysis method which gives an accumulative stress and bow values across the entire metal film (wafer surface), in XRD, typically, small areas of films are analyzed, and the result reflects stress inside smallest grains (via changes observed in lattice spacing when cooling and heating cycles are performed). The two techniques can be complementary, as the measured stress values show different stress effects at different scales. Both WLI and stage autofocusing function (of e.g. an ellipsometer) can be used for wafer curvature estimation, and, thus, identification of residual stresses after completion of thermal cycling. It is, however, challenging to use these techniques in combination with heating and cooling stages for *in situ* stress-temperature characterization.

In addition to experimental methods for stress measurement, to some extent, evaluation of thermal hysteresis can be achieved by FEM of MEMS components through optimization of dimensions and proximity of metal structures to any stress-sensitive elements [1,2]. However, it is challenging to include correct information about viscoelastic deformation occurring in metal films in this modelling method. Due to the complex interrelation of multiple effects causing mechanical stress in MEMS, correct interpretation of modelling data is difficult without detailed knowledge of the actual temperature dependent stress properties of films. In addition, even if stress can be reduced by optimization of design, Al structures often cannot be placed too far out relative to sensitive elements without compromising the electrical signal stability. Film stress has also been studied by micromachined test structures, such as cantilevers, suspended beams and membranes in various design configurations besides FEM modelling [13]. More theoretical and experimental background for analysis of stress in thin metal films can be found elsewhere [14-18].

C. *Formation of hillocks and voids in thin metal films*

Typically, hillocks and voids are formed on the surface of metal lines during the post-deposition annealing steps. Al is prone to hillock and void formation due to high mobility of atoms at elevated temperatures. Control of hillocks formation and protrusions through metal film is important as they may cause short circuits in electric circuits or disturb the integrity of the metal passivation layer in further processing steps. Formation of hillocks and voids is also an indication of mechanical stress appearing due to the mismatch in coefficients of thermal expansion (TCE) of metal film and other deposited films and the substrate. In the context of this work, analysis of formation of hillocks and voids on metal surface is important for two main reasons – integrity of the metal passivation layer during bulk Si etching and management of thermomechanical stress. Type of metal (specifically, their behavior in relation to thermo-mechanical properties such as elastic modulus, yield constants, etc.), sputtering and annealing conditions, thicknesses of film and substrate, type of substrate and presence of other thin films (oxides, nitrides, etc) influence the metal surface topography [19]. Presence of a second, thermo-mechanically more stable capping layer, e.g. Ti, in combination with Al, was shown to suppress hillock formation [20]. Thickness ratio of metal films combined in a stack is also an important parameter. Similarly, in Al-Ti alloys even a modest percentage of Ti may result in suppressed movement of grain boundaries thus, suppressing formation of hillocks and voids.

D. *Objectives of this work*

In the present contribution, we focus on characterization of mechanical stress and thermal hysteresis in sputtered Al, Ti, Al-Ti stacks and Al-Ti(1.8%Ti) alloy thin films by applying thermal cycling. Films of pure Al and pure Ti were used for reference while 1.8% Ti in Al alloy and stacks of Al/Ti films (thickness ratios of 1:1, 1:2, and 1:4, and both Al on Ti and Ti on Al) were evaluated as possible candidates to replace standard Al in the metallization processing step. The main objectives of this work are to compare these metal systems in terms of:

- Stress hysteresis behavior within the temperature range relevant for industrial pressure sensor applications;
- Surface morphology and microstructure (grain size, presence of hillocks and voids);
- Processing and integration aspects (wet etching, suitability for passivation with masking layer, suitability for wire bonding).

II. Experimental

A. Metal deposition

Two types of wafers were used in this study: 1) (100) p- Si wafers, double-side polished with thickness of 400 µm and 2) (100) p-type Si wafers, single-side polished with thickness of ca. 675 µm. The first type was used for *in situ* temperature-stress measurements and the second type for characterization of surface topography and TMAH etching tests.

All wafers were oxidized in dry oxygen to a nominal thickness of 1500 Å. Metal films of pure Al, stacks of Ti and pure Al (thickness ratios of 1:1, 1:2, and 1:4, and both Al on Ti and Ti on Al), and Al with 1.8% Ti with nominal thickness of 0.8 µm were sputter deposited on oxidized wafers using an MRC 643 and an AMAT (Applied Materials) Centura sputtering systems. After metal film deposition, selected wafers were sintered at 350 ˚C in forming gas 30 minutes.

Several selected test wafers were used for stress analysis and surface morphology as discussed in the following sections. However, not all wafers went through the same characterization procedures due to the lack of time and resources.

B. Measurement of stress

The measurements were performed using Flexus 2320S (Toho, USA) system located at Fraunhofer IZM, Department WLSI (Berlin, Germany). The wafer warpage method is illustrated in Figure 1. Each tested wafer was placed into a heating chamber on three pins where it rested throughout the entire measurement cycle. The chamber is purged with nitrogen gas during the measurement to prevent fast oxidation of studied metal films. The laser scans over the wafer. Data from ca. 80% of the wafer diameter is used in calculation of stress to exclude any stress inhomogeneity at the wafer edge. Accuracy of warpage measurement is approx. 1 MPa. To identify correctly the stress in deposited films, differential measurements are required, and initial stress of the substrate must be considered. In our case, it was not possible to scan wafers prior to the deposition of metal films. Therefore, each wafer was scanned twice in this sequence: 1) after completion of metal deposition and, if applicable, annealing processes, and 2) after completion of stress measurements and etching of the deposited metal film(s). The Stoney's equation (Eq. 1) was used to calculate the stress of deposited films [21].

$$\sigma_f = \frac{E_s d_s^2}{6(1-\nu_s)R d_f}, \quad (1)$$

where σ_f - stress of the deposited film, E_s and ν_s - Young's modulus and Poisson's ratio of the substrate, R - bending radius, d_s and d_f – thicknesses of substrate and deposited film, respectively.

TABLE I. Overview of the samples and corresponding thermal cycling conditions.

Sample ID**	Metal	Test protocol
Sintered at 350 ˚C before thermal cycling		
#1	0.8 µm Al	RT* – 200 ˚C – RT – 200 ˚C – RT – 150 ˚C (2 hr hold) – RT – 85 ˚C (2 hr hold) – RT
#2	0.8 µm Ti	RT – 200 ˚C – RT – 200 ˚C –RT – 150 ˚C (2 hr hold) – RT – 85 ˚C (2 hr hold) – RT
#3	0.4 µm Al + 0.4 µm Ti (Al on top)	RT – 200 ˚C – RT – 200 ˚C –RT – 150 ˚C (2 hr hold) – RT – 85 ˚C (2 hr hold) – RT
#4	0.8 µm Al-Ti (1.8 %Ti)	RT – 200 ˚C – RT – 200 ˚C –RT – 150 ˚C (2 hr hold) – RT – 85 ˚C (2 hr hold) – RT
#5	1 µm Al + 0.15 µm Ti (Ti on top)	RT – 200 ˚C – RT – 200 ˚C –RT – 150 ˚C (2 hr hold) – RT – 85 ˚C (2 hr hold) – RT After 3 weeks storage: RT – 150 ˚C (2 hr hold) – RT – 85 ˚C (2 hr hold) – RT
#6	0.6 µm Al + 0.35 µm Ti (Al on top)	RT – 200 ˚C – RT – 200 ˚C –RT – 150 ˚C (2 hr hold) – RT – 85 ˚C (2 hr hold) – RT After 3 weeks storage: RT – 150 ˚C (2 hr hold) – RT – 85 ˚C (2 hr hold) – RT
#7	0.8 µm Al	RT – 50 ˚C (2 hr hold) – RT – 85 ˚C (2 hr hold) – RT – 150 ˚C (2 hr hold)
#8	0.8 µm Al-Ti (1.8 %Ti)	RT – 50 ˚C (2 hr hold) – RT – 85 ˚C (2 hr hold) – RT – 150 ˚C (2 hr hold)
#9	0.8 µm Al-Ti (1.8 %Ti)	RT – 200 ˚C – RT – 200 ˚C –RT – 150 ˚C (2 hr hold) – RT – 85 ˚C (2 hr hold) – RT
Not sintered before thermal cycling		
#10	1 µm Al	RT – 450 ˚C – RT, the cycle repeated twice
#11	1µm (Al+Ti) (Al on top, ca. Al:Ti=2:1)	RT – 450 ˚C – RT, the cycle repeated after etching of Al

*RT – room temperature.

** All metal films were sputtered on Si (400 µm) substrates with SiO_2 (1500 Å). For #1–#4 was used Centura and for #5–#11 MRC 643 sputtering systems. More details are provided in *section A* of *Experimental*.

C. Analysis of sintered metal films

Below are summarized the analyses performed (for the test wafer, metal and test protocol descriptions see Table 1):

- Stress-temperature and stress-time behavior in the temperature range 25–200 ^{0}C: the test wafers #1 to #6 and #9 were subjected to the RT–200–RT–200–RT–150–RT–85–RT ˚C cycling sequence at heating and cooling rates of 5 ˚C / min, with a 2 hr hold time at 150 and 85 ˚C.

- Effect of wafer storage on stress at RT for up to three weeks: for the test wafers #5 and #6 the measurements were repeated 3 weeks later, only the curves with 150 and 85 ˚C maximum temperature and a hold time of 2 hr at each temperature.
- Effect of thermal cycling sequence and maximal temperature in each cycle on stress hysteresis: test wafers #7 and #8 were subjected to the cycling procedure with increasing maximum temperature in each consequent heat cycle, i.e. RT–50–RT–85–RT–150–RT ˚C with the hold time of 10 hr at maximum temperature in each cycle (50, 85 and 150 ˚C).
- Stress relaxation at elevated temperatures: measurements collected during 2 hr and 10 hr hold times at the respective temperatures (at 50 ^{0}C (#7, #8), 85 ^{0}C and 150 ^{0}C (#1 to #6 and #9)) were used for estimation of the time-dependent relaxation effects.

To compare measured curves, maximum hysteresis values and corresponding temperatures at which it occurred, change in residual stress at room temperature after completion of heat-cool cycle were calculated (for summary see Table 2).

D. Analysis of non-sintered metal films

Two test wafers (#10 and #11 in Table 1 and Figure 3) that did not undergo sintering were thermally cycled and analysed in terms of their stress-temperature and stress-time behaviour at RT – 450 ˚C – RT, at heating and cooling rates of 5 ˚C / min. The wafer #1 with standard Al was thermally cycled twice to identify the influence of the subsequent thermal cycle. For the wafer #2 with Al-Ti stack, the measurements were taken before and after etching of the top Al layer to identify individual contributions to stress hysteresis for both Al and Ti.

E. Surface characterization

A high-resolution scanning electron microscope (HRSEM) of type Quanta 600 FEGi (FEI) was used for metal surface imaging before and after sintering. HRSEM was operated in high vacuum, secondary electron (SE) detection mode with accelerating voltage of 10-20 kV and spot size 3. Magnification within x5.000 to x50.000 was applied. Images were taken in the central as well as close-to-edge areas. The height of hillocks and the depth of voids were estimated by cross-sectional analysis (tilting was used). The size of grains was studied in high-magnification SE and backscattered electron detector (BSD) modes, which in some cases, allowed for higher grain boundaries contrast. The goals for HRSEM analysis were to observe the difference of surface topography for different metal systems. Additionally, the goal was to identify influence of ratio of metal thicknesses as well as order of deposition on surface morphology for the Al-Ti stacks (Al:Ti thickness ratios of 1:1, 1:2, and 1:4, and both Al on Ti and Ti on Al).

F. Metal etching, passivation and testing of nitride mask layer

A standard Al etchant was used to etch Al and Al-Ti alloy. Ti was etched using the following solution H_2O:H_2O_2:(50%): HF20:1:1. The etched metal test structures for PECVD

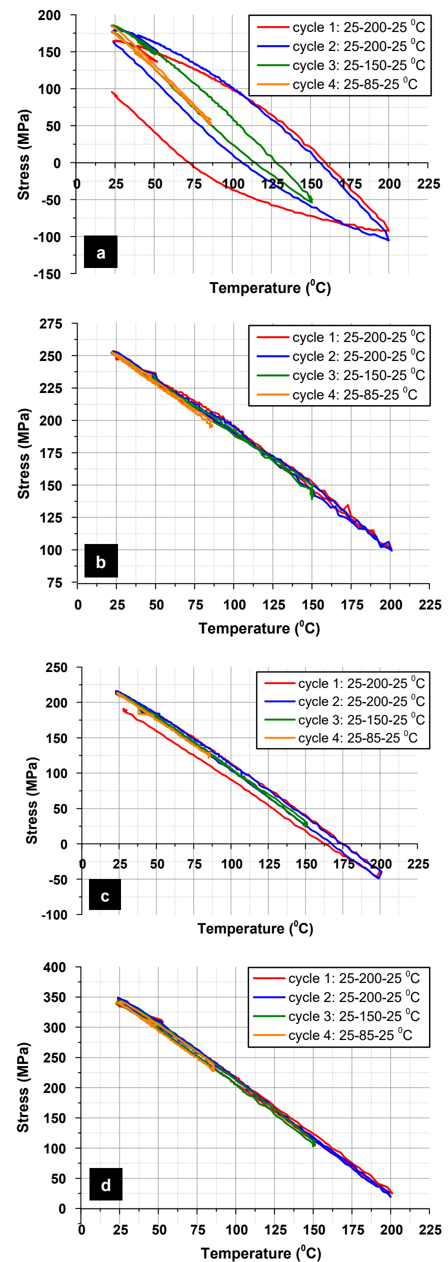

Fig. 2. Comparison of four metals (sintered) – Al (A), Ti (B), Al-Ti stack, 1:1 thickness ratio with Al on top (C) and Al-Ti alloy (D), referred as samples #1 to #4 in Table 1, respectively – studied in four thermal cycles up to 200, 150, and 85 ˚C.

passivation (1 µm thick) and tetramethylammonium hydroxide (TMAH) etching (over 20 hr) were manufactured using either 1- or a 2-mask process – patterning of contact holes and metal lines. In the case of 1-mask process only metal patterning was performed prior to nitride passivation, and contact pads were only in contact with oxidized Si surface. In the case of two mask process, 1500 Å SiO_2 was wet etched in BuHF (buffered oxide etch) solution through the photoresist mask (the etch time was 1 min 45 sec). Etch rate Si (100) in 25%TMAH at 70^{0}C was estimated to be approx. 15 µm / hr, and the etch rate of nitride passivation mask approx.10 nm / min. Both types of samples were sintered, passivated and subjected to TMAH

solution. The experiment aimed for selective etching of Si (210 µm deep Si etch) in TMAH for over 20 hours while keeping the nitride passivated metal lines and pads intact.

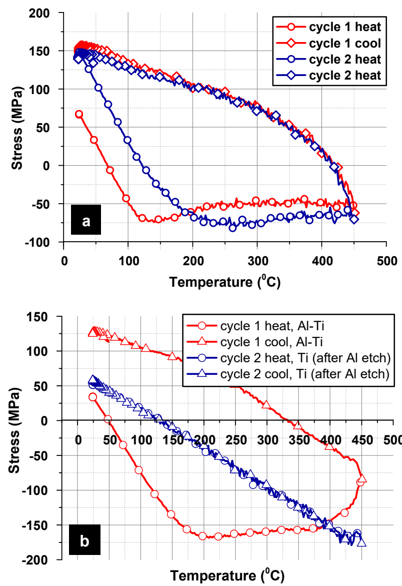

Fig. 3. Stress-temperature curves for non-sintered Al (a, sample #10 in Table 1) and Al-Ti (b, sample #11 in Table) collected within the temperature range RT–450˚C.

III. Results

A. Stress-temperature behaviour and thermal hysteresis in sintered metal films between RT and 200 ˚C

Figure 2 shows a comparison between the stress-temperature curves for four studied metals deposited in AMAT (Applied Materials) Centura sputtering system (#1 to #4). When comparing the first three heat-cool cycles (two between RT and 200˚C, followed by one between RT and 150˚C), the largest hysteresis values were observed for Al (35.40 – 129.98 MPa) and Al-Ti stack (16.62 – 42.72 MPa), followed by Al-Ti alloy with hysteresis in the range of 10 MPa. The lowest hysteresis was measured for Ti film (below 10 MPa). As a general trend, maximum of thermal hysteresis typically appears between 80 and 100 ^{0}C for all studied sintered metals. The hysteresis value decreases after subsequent cycles to the same target temperature or lower. All four metals show relatively low hysteresis (around or below 10 MPa) in the fourth heat-cool cycle up to 85 ˚C. The difference in residual stress at RT after completion of heat-cool cycle followed the same trend, i.e. the highest values observed for standard Al, followed by Al-Ti stack and Al-Ti alloy, lowest values for Ti. Absolute residual stress value at RT was measured to be the highest for Al-Ti alloy (up to 325-350 MPa), followed by Ti (approx. 250 MPa), and then Al-Ti stack (approx. 200 MPa) and standard Al (100 – 180 MPa).

B. Stress-temperature behaviour of non-sintered films from RT to 450 ˚C

In Figure 3 is shown the stress-temperature curve for standard Al (sample #1). Plastic deformation observed around 120 °C for the first heat-cool cycle and shifts towards 220 °C for the consecutive cycle. The maximum thermal hysteresis is approx. 200 MPa and observed at 129 ˚C. After the completion of first cycle, the residual stress change at RT is estimated to be approx. 91 MPa. After completion of the second cycle the maximum hysteresis value was decreased (approx. 176 MPa) and appeared at higher temperature (232 ˚C). The difference in residual stress value at RT after the second cycle was nearly 0 MPa. Larger thermal hysteresis value was observed for Al-Ti stack sample (#2) – approx. 249 MPa. The difference in residual stress after completion of the first cycle is comparable to standard Al (#1) – approx. 94 MPa. After etching of Al and repeated measurement of the #2 with the remaining Ti film, a nearly linear dependence with significantly lower hysteresis was measured (15.9 MPa). As in the case of #1, #2 showed nearly no change in residual stress value after completion of the second cycle (Ti film).

C. Deposition temperature

The ranges of elastic and plastic deformation are dependent on the deposition parameters, specifically, deposition temperature. Using temperature sensitive stripes, the temperature in MRC 643 was estimated to be approx. 80–120˚C for standard deposition conditions and found to be dependent on the number of deposition runs during the day. For the Centura sputtering system the deposition temperature is expected to exceed 100 °C based on the grain size analysis (large, developed grains of > 1 µm) for as deposited films (see below section H and Figure 9).

D. Stress relaxation at RT, 50˚C, 85˚C and 150 ˚C

- RT: change in residual stress close to RT (here 25 ^{0}C taken for comparison) can be noticed when multiple heat-cool cycles are performed on the same samples (e.g. two cycles of 200 ˚C) for all four metals. The effect is larger for Al and Al-Ti stack. The difference in residual stress typically decreases more than twice upon immediate application of consequent annealing cycles. Storage (for more than 2–3 hours) at RT led to further stress relaxation and, thus, increased change in residual stress values at RT. It may also lead to the increased maximum hysteresis value for follow up cycles.
- 50˚C, 85˚C and 150 ˚C: the largest stress relaxation effects were observed for Al standard at 150 ˚C (over 27 MPa within the first 4 hours at this temperature). The general trend of higher relaxation values at higher hold temperatures was observed for all metals (e.g. for Al standard 2-3 MPa within the first 4 hours at 85 ˚C and 1.2 MPa within the first 4 hours at 50 ˚C). For comparison with standard Al, Al-Ti alloy shown ca. 0.7 MPa at 50 ˚C, 1.3 MPa at 85 ˚C and 5 MPa at 150 ˚C (in each case total hold time of 10 hr was used).

E. Effect of wafer storage

Figure 4 shows the stress-temperature curves collected from the test wafers with different ratio of thicknesses of Al and Ti (samples #5 and #6, Table 1) before and after three weeks of

storage. Higher hysteresis value after 3 weeks storage was observed for the sample # 5 (thicker Al film), i.e. approx. 50 MPa compared to approx. 30 MPa measured initially in RT–150 ˚C. This effect was not observed for the same sample in RT–85 ˚C cycle. Sample #6 indicated slight increase in the maximum hysteresis value in both curves (RT–150 ˚C and consequent RT–85 ˚C cycles).

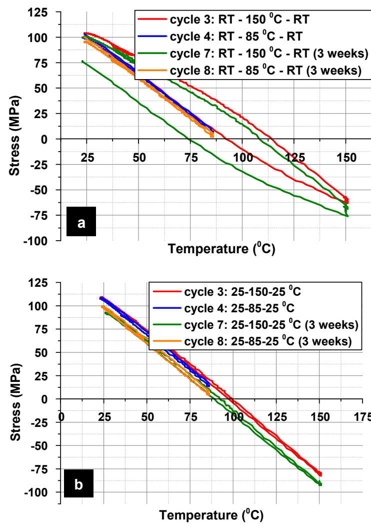

Fig. 4. Stress-temperature curves showing the effect of 3 weeks storage on maximum hysteresis and residual stress for two Al-Ti stack samples #5(a) and #6 (b).

F. *Effect of thermal cycling sequence and maximum temperature in cycle*

Figure 5 shows the curves collected on the test wafers with Al and Al-Ti(1.8% Ti) alloy (#7, #8, #9 in Table 1) sputtered in the same equipment (MRC 643). The effect of thermal cycling sequence was observed by changing the order of applying cycles with "high" (150 or 200 ˚C) and "low" (50 or 85 ˚C) temperature in a cycle. For the case of increasing maximum temperature (Figure 5A and 5B), both Al standard and Al-Ti alloy show low hysteresis values for cycles up to 50 and 85 ˚C, i.e. less than 10 MPa (see Table 2). However, Al standard shows higher hysteresis at 150 ˚C (82.50 MPa) compared to Al-Ti alloy (26.98 MPa). Figures 5B and 5C correspond to the same material, i.e. Al-Ti alloy, but different thermal cycling sequence. Both curves collected for the cycles with maximum temperatures of 150 and 85 ˚C show roughly similar maximum hysteresis and residual stress values.

G. *TMAH etch test with PECVD nitride*

In the case of nitride passivation of metal structures (Figures 6 and 7) on oxidized Si all 4 metal systems – Al standard, Al-Ti(1.8%) alloy, Al-Ti stack and Ti – remained intact throughout the 23 hr etch test in TMAH solution. PECVD nitride passivation for metals on non-oxidized Si surfaces initially gave desired results for three metal systems – Al-Ti(1.8%), Al-Ti stack and Ti which was concluded after 19.5 hr etch in TMAH solution. Al standard showed some degradation of metal lines after 17 hr, however, this was not attributed to the presence of hillocks on the surface.

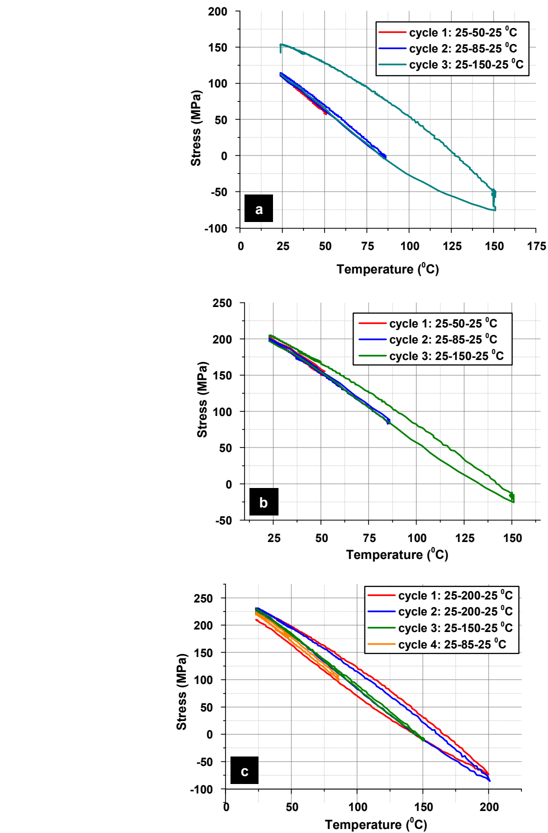

Fig. 5. Stress-temperature curves showing the effect of thermal cycling sequence on maximum hysteresis and residual stress for Al (# 7(a) and Al-Ti alloy b(#8) and c(#9)).

The repeated etch tests with Al standard and nitride passivation gave satisfactory results during the target 20 hr in solution. In summary, Al standard on non-oxidized Si surfaces has the highest risk of failure during Si etching with protective nitride passivation due to the highest number and size of hillocks.

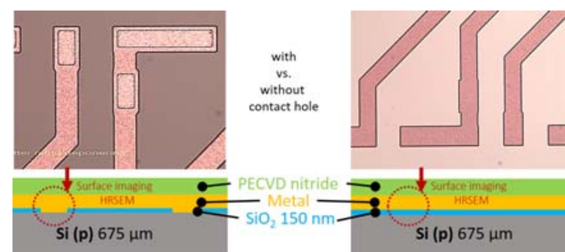

Fig. 6. Optical microscopy images and schematic cross-sectional views of the test structures used in PECVD and TMAH etching tests.

H. *HRSEM surface imaging*

Larger hillocks and higher number of hillocks was found on surfaces where metal is in direct contact with Si compared to oxidized Si surface. Figure 7a shows an overview of metal contact pads for the studied metal systems with clear appearance of large hillocks in the openings to Si for Al standard and Al-Ti alloy. Figure 7b and 7c show close-up images of typical hillocks found on Al standard surface.

Patterning of metal films did not have any effect on surface topography for both sintered and non-sintered films. In the case of Al-Ti stack an extra etching step of Ti is required. An under-etch of a few microns and rough edge for Ti was observed (Figure 9). We believe this can easily be improved by a fine-tuning of the etching solution and time [22], as well as compensated by design.

Figure 9 shows a surface morphology comparison between the studied metal systems before and after sintering. Standard Al indicated large (up to a few microns in width) and well-developed grains even for as-deposited films. Al-Ti alloy exhibits smaller grains compared to standard Al. The results of the surface imaging are in line with the stress-temperature curves for both metals (Figure 2): higher residual stress at RT for Al-Ti alloy which also remains stable after cycling. For Al-Ti stack films, the morphology found to be dominated by Al (specifically for 1:1 thickness ratio and when Al is thicker than Ti). Ti surface did not show any voids or hillocks after sintering.

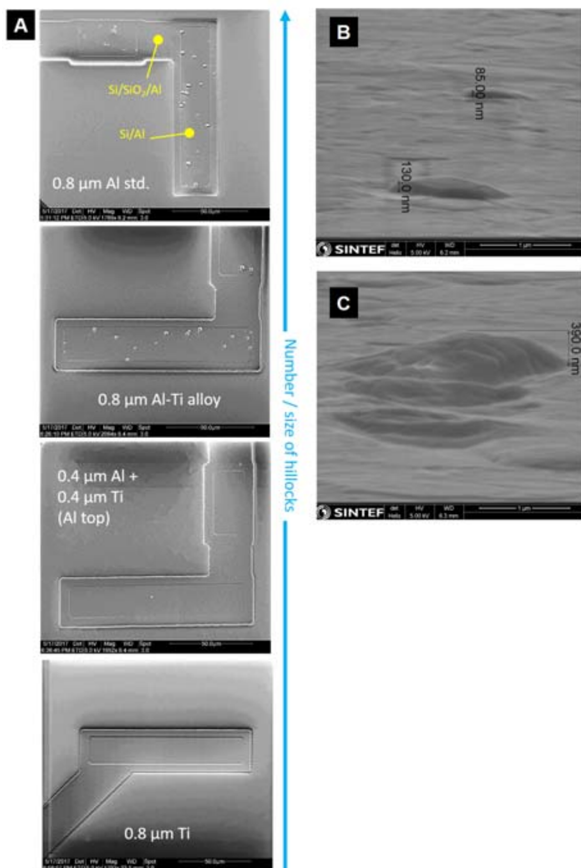

Fig.7. HRSEM images showing the contact areas of the test structures (A) where the arrow pointing towards samples with highest number and largest hillocks; and typical dimensions of hillocks on standard Al formed on Si/SiO_2 substrate (B, C).

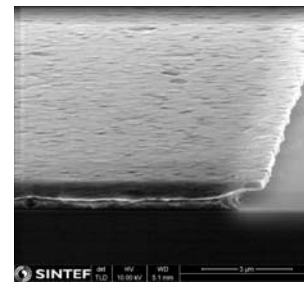

Fig. 8. HRSEM image of Al-Ti stack (Al on top) film after metal patterning and showing under etch in Ti.

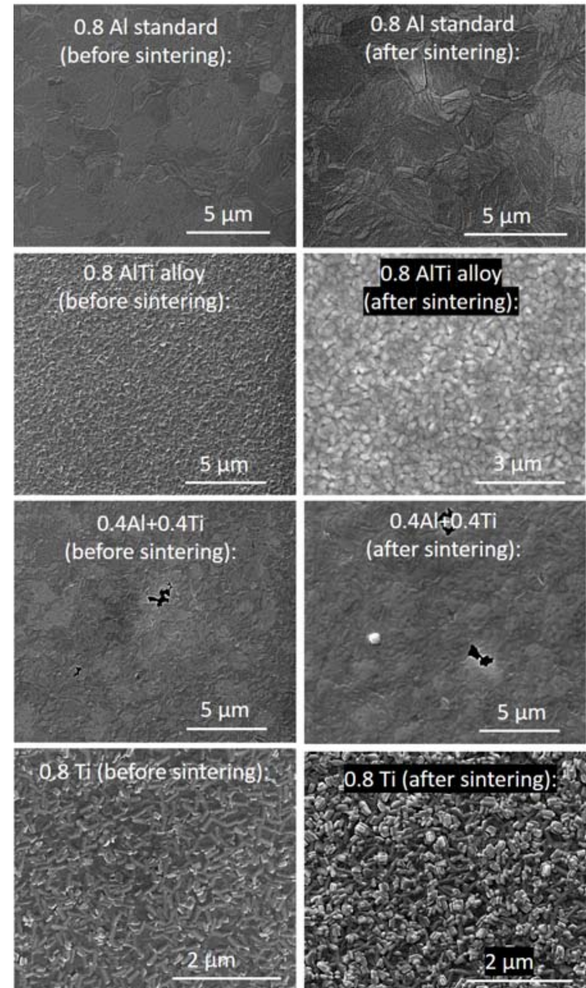

Fig. 9. HRSEM images taken before and after sintering at 350 ˚C. The films were deposited using Centura sputter tool, but the results correspond well to the films from the MRC 643 sputter tool.

IV. DISCUSSION

A. *Comparison of stress and thermal hysteresis properties of Al, Al-Ti stack, Al-Ti(1.8%) alloy and Ti films*

For the application in pressure sensors with two target temperatures – 85 ^{0}C and 150 ^{0}C, both Al-Ti stack and Al-Ti alloy show minimal hysteresis and can perform well as metallization layer. Both a Ti capping layer and incorporation of Ti into Al matrix suppresses extensive grain boundaries movement and relaxation processes occurring in softer Al.

Al standard may still be a reliable alternative after conditioning (long-term annealing or thermal cycling) if the target temperature range for device operation is from RT to 85 ˚C. As shown in Figures 2, 4 and 5, hysteresis is minimal in this temperature range. Al-Ti stack and Al-Ti alloy are the preferred metals if broader temperature range is required.

Absolute value of residual stress is an important parameter. Although Al-Ti alloy demonstrated promising properties in terms of thermal hysteresis, it also demonstrated high residual stress at RT. The lowest values of residual stress at RT were found for Al, however, Al also showed the most pronounced change in residual stress after cycling compared to other metals.

The stress-temperature curves collected for non-sintered standard Al and are in line with literature, both in terms of total hysteresis values and residual stress. Most of the processes related to grain reorganization are completed in the first thermal cycle. The results of stress measurements correlate well with surface imaging analysis. As deposited metal film is not in thermo-dynamic equilibrium and the grain size changes with sintering, this change will be more pronounced for soft metals such as Al.

Unfortunately, both sputtering machines used in this study do not provide the possibility of in situ temperature control during deposition. There were multiple differences between the results obtained for the same materials sputtered in these two systems. For example, in the case of standard Al, much larger grains were found characteristic for films deposited in Centura compared to MRC 643, suggesting higher deposition temperature. The main effect on grain size difference is attributed to impurity level. The difference between 8e-7 and 2e-8 torr residual pressure is leading to a large difference in surface mobility. Figure 2D and 5C show both Al-Ti alloy corresponding to Centura and MRc 643, respectively. The test results for the test wafer from MRC 643 compared to Centura indicated larger hysteresis values, but significantly lower values of residual stress at RT.

Metal films exhibited both short- (a few hours) and long-term (up to 3 weeks in this study) relaxation effects. The general trend is that the observed effects are thermal history-dependent and were the largest for Al standard.

It was found that the order in which thermal cycles are applied has lesser influence on the total hysteresis and residual stress values than the maximum temperature in each cycle (the higher the temperature the larger hysteresis and residual stress change are expected).

B. Comparison of surface and microstructural properties of Al, Al-Ti stack, Al-Ti(1.8%) alloy and Ti films

Ti as a top layer can be used where hillock-free metal surfaces are required (hillock formation was suppressed within the studied ratio of thicknesses Ti-Al). In Al-Ti stack films with Al as a top layer (for example, due to wire bonding requirements), Ti thickness should be kept equal or larger than that of Al to achieve surface with lower number of hillocks and voids. Al(1.8%)Ti alloy can be a good alternative to metal surfaces with a lot of hillocks, e.g. Al standard, but cannot be considered completely hillock-free. The metal systems with the highest number of hillocks and voids are Al standard, and Al-Ti with Al on top and thicker than Ti. Large, developed grains found on the surface of Al standard suggest that temperature during deposition should be well above 100 ˚C. Smaller grain size range found for Al-Ti alloy and Al-Ti stack compared to Al standard can be explained by suppressed grain boundaries movement due to presence of more thermo-mechanically stable Ti.

V. Conclusions

Two metal systems were found to be promising alternatives to pure Al: 0.8 µm thick 1.8% Ti in Al alloy and 0.4 µm Ti / 0.4 µm Al (Al on top). These films exhibited lower hysteresis values (Figure 2, Table 2), considerably lower number of hillocks (Figures 7 and 9) and failure-free TMAH etch tests, and therefore considered for follow-up testing on the sensor level. Al-Ti alloy is a better choice in terms of material integration as it can be etched in the standard Al etchant in one step, but Al-Ti stack requires additional etching step. Completely hillock-free surfaces can be obtained in Al-Ti stack films with Ti on top and pure Ti films, however, wire bonding to Ti surface may be challenging.

TABLE II. Overview of the measured maximum hysteresis with corresponding temperature at which it appears and difference in residual stress after completion of a heat-cool cycle at room temperature.

Sample ID*	Metal	T_{max} in cycle (˚C)	Max hysteresis (MPa) / T at max hysteresis (˚C)	ΔResidual stress at RT, (MPa)
#1	0.8 µm Al	200	137.13 / 90	67.60
		200	92.83 / 103	15.16
		150	38.67 / 96	7.72
		85	9.32 / 30	8.35
#2	0.8 µm Ti	200	9.76 / 173	2.02
		200	7.16 / 152	1.60
		150	6.37 / 141	0.76
		85	4.12 / 83	0.51
#3	0.4 µm Al + 0.4 µm Ti (Al on top)	200	46.62 / 94	12.42
		200	34.30 / 107	0.10
		150	16.46 / 82	1.94
		85	3.05 / 76	0.1
#4	0.8 µm Al-Ti (1.8 %Ti)	200	12.20 / 91	9.77
		200	8.84 / 50	3.42
		150	11.36 / 105	7.09
		85	12.35 / 72	0.23
#5	1 µm Al + 0.15 µm Ti (Ti on top)	150	31.71 / 93	2.46
		85	5 / 24	3.21
		150	50.10 / 87	26.62
		85	4.68 / 24	3.62
#6	0.6 µm Al +	150	4.59 / 104	9.38

Sample ID*	Metal	T_{max} in cycle (˚C)	Max hysteresis (MPa) / T at max hysteresis (˚C)	ΔResidual stress at RT, (MPa)
	0.35 μm Ti (Al on top)	85	4.49 / 37	2.08
		150	6.70 / 86	3.49
		85	6.93 / 71	1.34
#7	0.8 μm Al	50	4.61 / 46	0.13
		85	7.57 / 52	4.06
		150	82.90 / 87	43.52
#8	0.8 μm Al-Ti (1.8 %Ti)	50	9.23 / 45	0.91
		85	6.25 / 61	2.29
		150	26.98 / 107	9.06
#9	0.8 μm Al-Ti (1.8 %Ti)	200	55.15 / 112	21.72
		200	36.97 / 136	3.36
		150	8.3 / 117	5.33
		85	8.79 / 48	3.55
#10	0.8 μm Al	450	198.98 / 129	90.95
		450	176.44 / 232	0.21
#11	0.8 μm Al	450	248.88 / 190	94.1
		450	15.9 / 358	4.12

* For #1–#4 was used Centura and for #5–#11 MRC 643 sputtering systems. More details are provided in section A of *Experimental*.

ACKNOWLEDGMENT

This research was supported by the Norwegian Research Council through the project NBRIX (247781). The authors acknowledge Martin Fleissner Sunding (SINTEF Industry) and Joachim Seland Graff (SINTEF Industry) for their help with HRSEM imaging. Vishnukanthan Venkatachalapathy (University of Oslo) is greatly acknowledged for discussions on stress characterization in thin metal films.

REFERENCES

[1] J.A. Chiou, S. Chen, "Thermal hysteresis and voltage shift analysis for differential pressure sensors", Sensor Actuat.A-Phys., Vol. 135, No.1, pp.107–112, 2007.

[2] J.A. Chiou, S. Chen, "Thermal hysteresis analysis of MEMS pressure sensors", J. Microelectromech.S., Vol.14, No.4, 2005.

[3] Å. Sandvand, E. Halvorsen, H. Jakobsen, "In situ observation of metal properties in a piezoresistive pressure sensor", J. Microelectromech. S., Vol.26, No.6, pp.1381–1388, 2017.

[4] H.-N. Chiang, T.-L. Chou, C.-T. Lin, K.-N. Chiang, "Investigation of the hysteresis phenomenon of a silicon-based piezoresistive pressure sensor," in Proceed. of International microsystems, packaging, assembly and circuits technology, Taipei, 2007, pp. 165–168.

[5] H. Windischmann, "Intrinsic stress in sputter deposited thin films", Crit. Rev. Solid State, 17, pp. 547–596, 1992.

[6] D.S. Gardner, P.A. Flynn, "Mechanical stress as a function of temperature in aluminum films", IEEE T. Electron Dev., 35, pp. 2160–2169, 1988.

[7] J.A. Thornton, D.W. Hoffmann, "Stress-related effects in thin films", Thin Solid Films, 171, pp. 5–31, 1989.

[8] P.A. Flinn, D.S. Gardner, W.D. Nix, "Measurement and interpretation of stress in aluminium-based metallization as a function of thermal history", IEEE Electron. Dev., Vol. ED-34, No. 3, 1987.

[9] E. Eiper, R. Resel, C. Eisenmenger-Sittner, M. Hafok, J. Keckes, "Thermally-induced stresses in thin aluminium layers grown on Si", in proceed. JCPDS 2004, pp. 368–372, 2004.

[10] E. Eiper, J. Keckes, K.J. Martinschitz, I. Zizak, M. Cabié, G. Dehm, Size-independent stresses in Al thin films thermally strained down to −100°C, Acta Materialia, Vol. 55, No. 6, 2007, pp. 1941–1946.

[11] E. Vereshchagina, E. Poppe, K. Schjølberg-Henriksen, V. Venkatachalapathy, S. Moe, "Analysis of residual stress and thermal hysteresis in sputtered Al thin films", in Proceed. Micromechanics Europe 2014, 1–3 September, Istanbul, Turkey, 2014.

[12] A. Segrnueller, Murakami, M., “X-Ray diffraction analysis of strains and stresses in thin films”, in Treatise on Materials Science and Engineering, Vol.27, H., Herman, ed., Academic Press, New York, 1988, pp. 143–200.

[13] L. Elbrecht, U. Storm, R. Catanescu, J. Binder, "Comparison of stress measurement techniques in surface micromachining", J. Micromech. Microeng., 7 pp. 151–154, 1997.

[14] J.H. Jou, L. Hsu, "Stress analysis of elastically anisostropic bilayers structures", J. Appl. Phys., Vol. 69, No. 3, pp.1384–1388, 1991.

[15] W.D. Nix, "Mechanical properties of thin films", Metall. Trans. A, Vol. 20A, pp.1989–2217, 1988.

[16] R.P. Vinci, E.M.Zielinski, J.C. Bravman, "Thermal stress and strain in copper thin films", Thin Solid Films, Vol. 262, pp. 142–153, 1995.

[17] C.D. Graas, "Stress-related phenomena in capped al-based metallizations", Mater. Res. Soc. Sym. Proceed., Vol. 200, 1992.

[18] M.Hershkovitz, A.Blech, Y.Komem, "Stress relaxation in thin Al films", Thin Solid Films, Vol.130, No. 1-2, pp.87–93, 1985.

[19] D. Resnik, J. Kovac, M. Godec, D. Vrtacnik, M. Mozek, S. Amona, "The influence of target composition and thermal treatment on sputtered Al thin films on Si and SiO2 substrates", Vol. 96, pp.29–35, 2012.

[20] K.-H. Jang, S.-J. Hwang, Y.-C. Joo, “Effect of capping layer on hillock formation in thin Al films”, Met. Mater. Int., Vol. 14, No.2, pp. 147–150, 2008.

[21] L. B. Freund, S. Suresh, "Thin Film Materials: Stress, Defect Formation and Surface Evolution", 2003, Cambridge University Press.

[22] M. Shikida, K. Sato, K. Tokoro, D. Uchikawa, "Differences in anisotropic etching properties of KOH and TMAH solutions", Sensor Actuat. A:Phys, Vol.80, No.2, pp.179–188, 2000.